ACS APPLIED MATERIALS & INTERFACES

Research Article

Cite This: ACS Appl. Mater. Interfaces 2018, 10, 34502−34512

www.acsami.org

High-Performance Graphene-Based Natural Fiber Composites

Forkan Sarker,[†,‡,⊥] Nazmul Karim,[*,∥,⊥] Shaila Afroj,[§,∥] Vivek Koncherry,[†,‡] Kostya S. Novoselov,[§,∥] and Prasad Potluri[*,†,‡]

[†]School of Materials, [‡]Northwest Composites Centre, and [§]School of Physics & Astronomy, The University of Manchester, Oxford Road, Manchester M13 9PL, U.K.

[∥]National Graphene Institute (NGI), The University of Manchester, Booth Street East, Manchester, M13 9PL, U.K.

Supporting Information

ABSTRACT: Natural fiber composites are attracting significant interest due to their potential for replacing synthetic composites at lower cost with improved environmental sustainability. However, natural fiber composites suffer from poor mechanical and interfacial properties. Here, we report coating of graphene oxide (GO) and graphene flakes (G) onto natural jute fibers to improve mechanical and interfacial properties. The coating of graphene materials onto jute fibers enhanced interfacial shear strength by ∼236% and tensile strength by ∼96% more than untreated fibers by forming either bonding (GO) or mechanical interlocking (G) between fibers and graphene-based flakes. This could lead to manufacturing of high-performance and environmental friendly natural fiber composites that can potentially replace synthetic composites in numerous applications, such as the automotive industry, naval vessels, household products, and even in the aerospace industry.

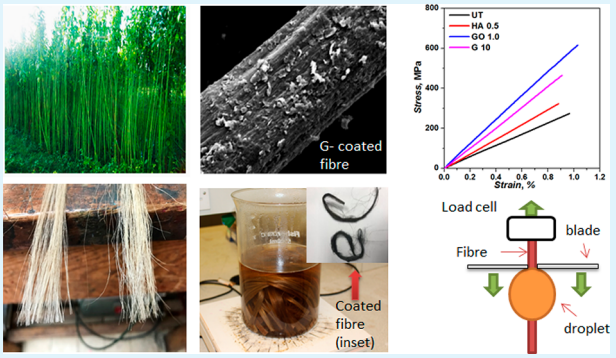

KEYWORDS: *natural fibers, jute fibers, composites, graphene, graphene oxide, interfacial shear strength and tensile properties*

INTRODUCTION

Natural fibers are becoming increasingly attractive to composite manufacturers and material scientists due to their lower environmental impact, such as less carbon emission and fossil fuel consumption, biodegradability, lower cost, lower density, and ease of fabrication.[1] The utilization of lightweight natural fibers such as jute, flax, kenaf, hemp, and sisal could potentially replace a large amount of glass and mineral fillers in numerous automotive and aerospace applications (Table S1, Supporting Information).[2] Flax, hemp, and jute are dominating natural fibers in the European automotive industry. Among them, jute fibers have attracted significant interest given that they may be able to replace glass fibers (GFs) partially or fully due to their lower specific gravity (∼1.3) compared to that of glass (∼2.5) and a higher specific modulus (∼40 GN/m^2) than that of glass (∼30 GN/m^2).[3] Moreover, jute is the second-most produced (mainly in Bangladesh, India, and China) natural fiber after cotton and is at least 50% cheaper than flax and other natural fibers.[4] However, jute fiber experiences lower mechanical properties and poor interfacial shear strength (IFSS) while reinforced with epoxy matrix, due to the presence of large amounts (20−50 wt %) of noncellulosic materials, such as hemicellulose and lignin (Table S2, Supporting Information). These noncellulosic materials are responsible for the lower crystallinity[5] and hydrophilic nature of jute fibers[6] and play an important role in determining the characteristic properties of fibers.

The alkali treatment of jute fiber usually removes noncellulosic materials, predominantly hemicellulose and some lignin.[7−10] Hemicelluloses are present in the interfibrillary region of jute fiber. The deformation of this fibrillary network[11] is mainly responsible for the stress development and relaxation in stretched jute fiber, whereas the lignin is located in the intercellular region and the behavioral change in that region plays a dominant role in determining tensile characteristics of jute fibers. The alkali treatment removes noncellulosic materials and impurities from the interfibrillar region of jute fibers, which makes the fibrils more capable of rearranging themselves along the direction of tensile deformation. This will allow fibrils to have a better load sharing capability between themselves to contribute in higher stress development during the tensile test.[12] While lignin is removed gradually, the middle lamella becomes more plastic as well as homogenous due to the gradual elimination of microvoids. As suggested in a previous study,[8] the treatment with a lower alkali concentration (∼0.5 wt %) for a prolonged time is an effective technique to enhance the mechanical properties of jute fiber. However, the enhancement is limited and not even close to glass fiber properties. Moreover, the treatment with a higher alkali concentration may reduce the hydrophilicity by

Received: August 1, 2018
Accepted: September 17, 2018
Published: September 17, 2018

DOI: 10.1021/acsami.8b13018
ACS Appl. Mater. Interfaces 2018, 10, 34502−34512

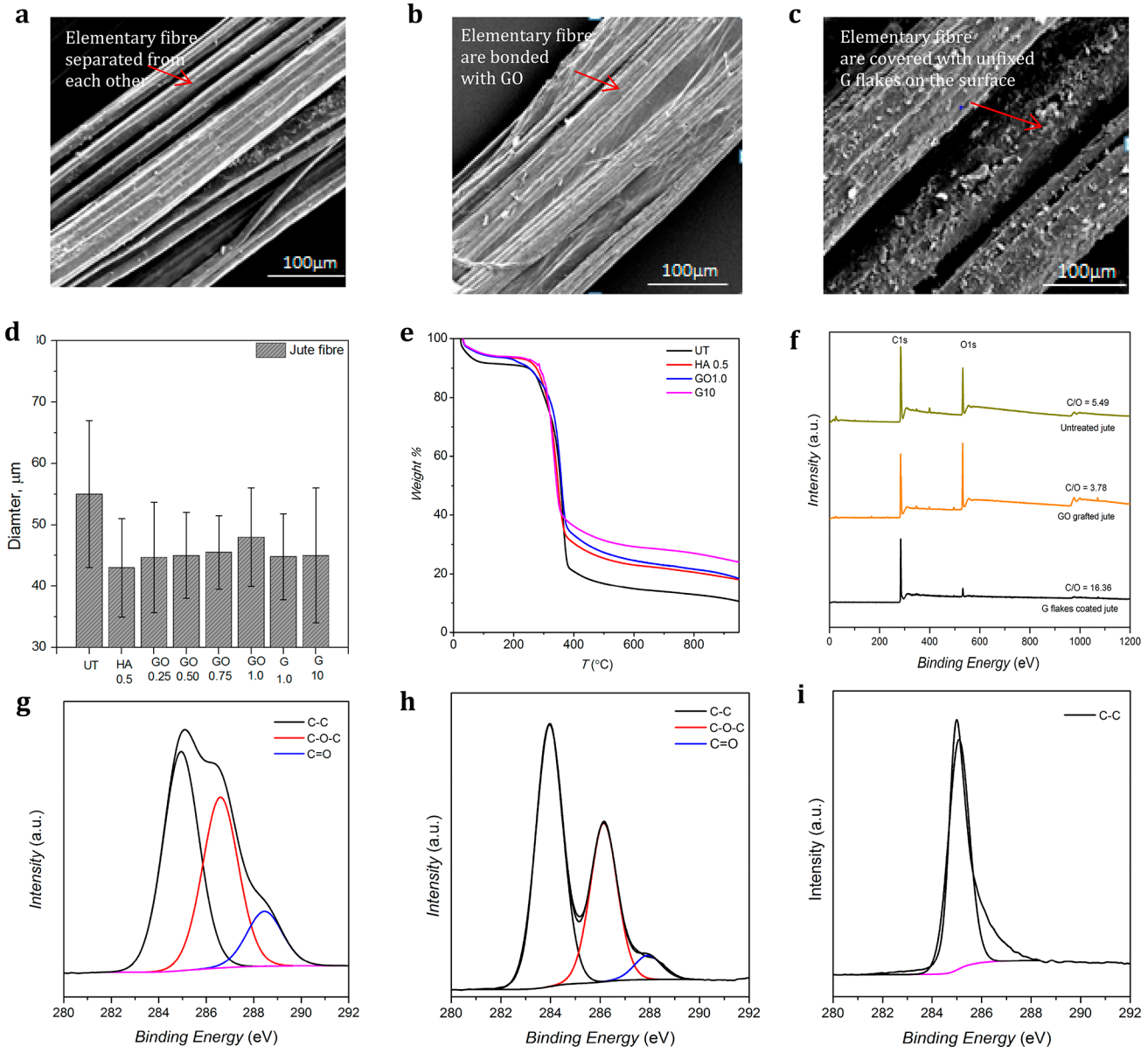

Figure 1. SEM images of (a) untreated jute fiber (X250); (b) GO-coated jute fiber (X250), and (c) G flake-coated jute fiber (X1500); (d) the diameter of untreated and treated jute fibers; (e) thermogravimetric analysis (TGA) curves for treated and untreated fibers; (f) wide-scan XPS spectra of untreated, GO, and G flake-treated jute fibers; (g) high-resolution (C 1s) XPS spectra of untreated jute fiber; (h) high-resolution (C 1s) XPS spectra of GO-coated jute fiber; and (i) high-resolution (C 1s) XPS spectra of G flake-coated jute fiber.

removing more hydroxyl components,[13] thus creating an adverse effect on the tensile and interfacial properties of jute composites.[14,15] Several studies[16,17] also reported surface treatment of alkali-treated jute fiber with organosilane[16] and plasma[18] to further improve interfacial shear strength; however, the improvement is not significant and some of the treatments are expensive and time consuming. Therefore, there remains a need for a new kind of surface treatment for jute fibers that could improve both tensile and interfacial shear strength significantly and potentially outperform glass fiber composites.

Graphene, a single-atom-thick sheet of hexagonally arrayed sp^2-bonded carbon atoms, has attracted tremendous attention for high-performance composite applications due to its incredible mechanical properties.[19] The graphite oxide route is the most attractive method for producing huge quantities of graphene materials such as graphene oxide (GO)[20] and reduced graphene oxide (rGO)[21] in stable forms. Moreover, GO sheets show good chemical reactivity and handling characteristics due to their intrinsic functional groups.[22] Furthermore, the scalable production of graphene flakes (G) by microfludization technique and their applications for making smart composites is demonstrated.[23] Recent studies[24−26] have reported improvement of the mechanical and interfacial properties due to the grafting of GO onto synthetic fiber surfaces such as carbon, glass, and poly(*p*-phenylene benzobisoxazole) (PBO). For example, interfacial shear strength (IFSS) has been increased by 70.8% by uniform coating of GO on a carbon fiber surface.[25] GO has also been coated covalently onto glass fibers (GFs) by amidation reaction[24] between the carboxyl groups of GO and the amino groups of amino-terminated GFs to improve the IFSS of glass/epoxy composites. Moreover, a GO coating on a (PBO) fiber surface with a silane coupling agent (KH-540) enhances

DOI: 10.1021/acsami.8b13018
ACS Appl. Mater. Interfaces 2018, 10, 34502−34512

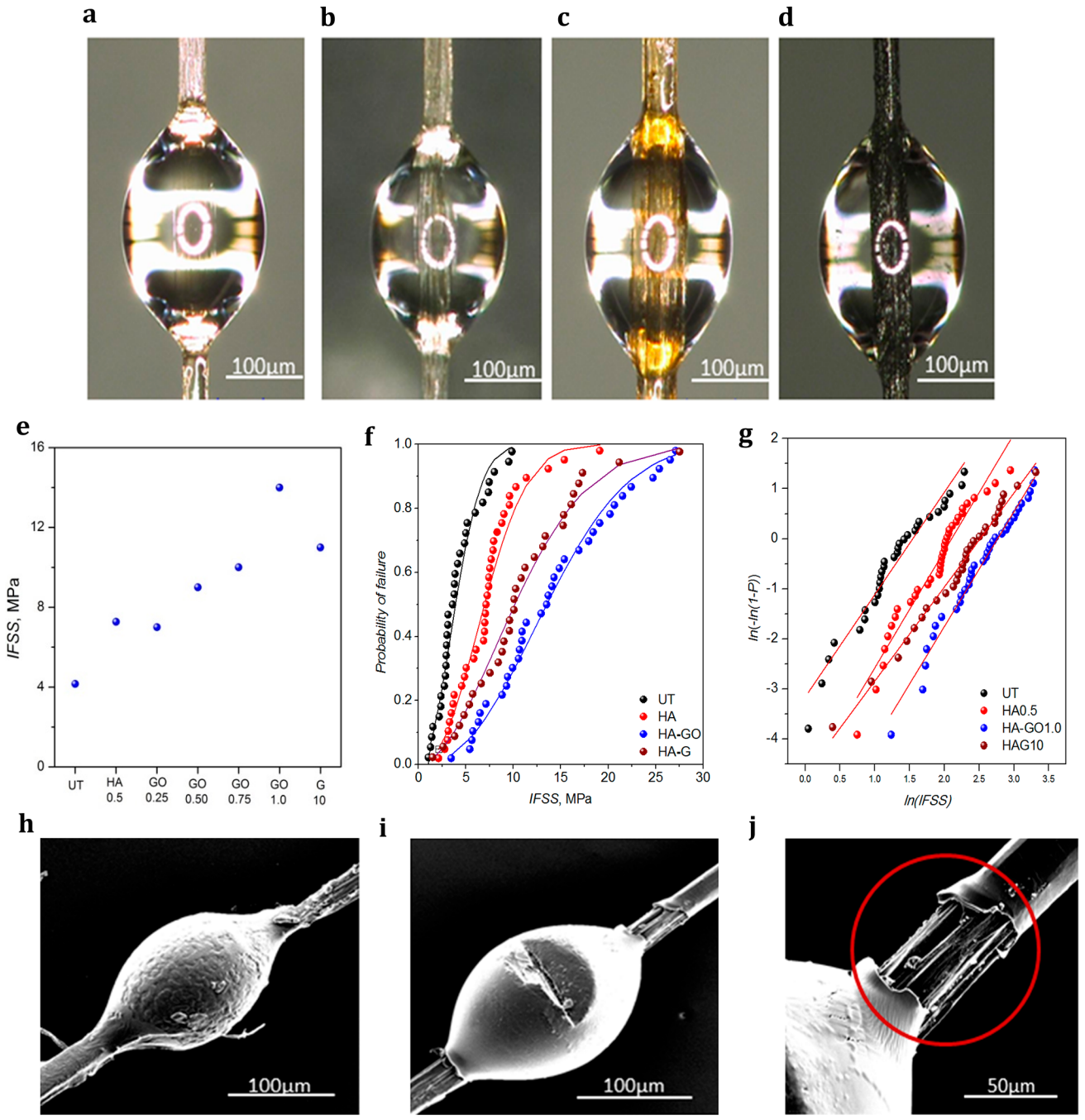

Figure 2. (a) Optical images of the microdroplet on (a) untreated jute fiber (X200); (b) HA 0.5-treated jute fiber (X200); (c) GO-coated jute fiber (X200); (d) G flake-coated jute fiber (X200); (e) interfacial shear strength (IFSS) of untreated, GO, and G flake-coated jute fibers; (f) interfacial shear strength data fitted to a two-parameter Weibull distribution as a function of surface treatment; (g) ln curve of Weibull parameter plot distribution considering interfacial shear strength; (h) SEM image of microdroplets of epoxy on jute fiber before microbond test (X250); (i) SEM image of microdroplets of epoxy on jute fiber after microbond test (X250), and (j) SEM image of debonded area (red circle line) after microbond test (X250).

IFSS by 61.6%.[27] Furthermore, the surface treatment of naturally derived fibers with nanofunctional materials is becoming an attractive choice to the researchers due to their biocompatibility and strong interfacial interactions with multiple reactive sites.[28−30] Although a very few studies reported grafting of nanoparticles such as $NanoTiO_2$[31] and ZnO_2[26] on natural fibers, no study has been found so far on coating graphene or graphene derivatives on commonly used natural fibers such as jute and flax.

Here, we report for the first time coating of graphene materials such as GO and G flakes onto alkali-treated jute fibers to improve mechanical and interfacial properties. The jute fibers were first treated with a lower concentration (0.5 wt % NaOH) of alkali to remove noncellulosic materials. The alkali-treated fibers were then coated uniformly with GO and G flakes. The surface characteristics of graphene-coated jute fibers were analyzed using scanning electron microscopy (SEM) and X-ray photoelectron spectroscopy (XPS). The change in fiber diameter was observed using an optical

DOI: 10.1021/acsami.8b13018
ACS Appl. Mater. Interfaces 2018, 10, 34502−34512

microscope. A microbond test was conducted to study the effect of GO and G flakes on the interfacial properties of jute/epoxy composites and also evaluate the mechanical properties of graphene material-coated jute fibers.

RESULTS AND DISCUSSION

Characterization of Coated Jute Fibers. Figure 1a−c shows SEM micrographs of untreated and coated jute fibers. Figure 1a shows SEM images of a smooth and featureless untreated jute fiber surface, which may be due to the presence of a cementing layer that is composed of waxes, fats, lignin, pectin, and hemicelluloses.[32] After heat and alkali treatment, the surface roughness of the jute fiber increases,[16] due to partial removal of that cementing layer (Figure S1, Supporting Information). Generally, a grooved appearance with microvoids is visible after the alkali treatment (Figure S1b, Supporting Information). The coating of GO shows a more uniform and evenly coated fiber surface with only a few flakes present on the surface (Figures 1b and S1c, Supporting Information), which may be due to chemical bonding provided by the functional groups of GO.[22] For graphene flakes (G 10), however, a uniform coating is achieved with plenty of unfixed graphene flakes being present on the fiber surface, shown in Figures 1c and S1d, Supporting Information. Moreover, the color of HA 0.5-treated jute fibers changes from brown to yellowish for GO and black for G flakes (Figure S2c,d, Supporting Information). The diameter of untreated jute fibers is found to be 55 ± 12 μm, shown in Figure 1d. After alkali treatment, we observe that the diameter of the jute fibers (HA 0.5) is reduced by 23.5% to 43 ± 8 μm, which is in agreement with previous studies.[8,33,34] The reduction of fiber diameter may be due to the removal of hemicellulose, pectin, and lignin.[14,16,35] However, coating of graphene materials onto HA 0.5-treated jute fibers shows an overall increase in the fiber diameter. As expected, the diameter of GO-coated fibers increases with the increase of GO concentration, shown in Figure 1d.

TGA analysis of untreated and graphene material-coated samples show that the thermal stability of jute fibers reduces after heat and alkali treatment, due to the removal of hemicellulose and lignin, shown in Figure 1e (and Table S3, Supporting Information). However, coating of graphene materials onto jute fibers improves their thermal stability by at least 11 °C, which is in agreement with a previous study.[36] This could be explained by the formation of a carbonaceous shield of graphene materials on the fiber surface,[37,38] which delays the degradation and improves thermal stability of the fiber. We use XPS analysis to characterize surface functionalities of untreated and graphene material-coated jute fibers, shown in Figure 1f−i. The wide-scan XPS spectra show that the C/O ratio of jute fibers decreases from 5.49 to 3.78 after coating with GO, due to the presence of oxygen-containing functional groups in GO,[20,22] whereas C/O ratio of G 10-coated samples increases to 16.36 after grafting graphene flakes onto jute fiber surfaces, due to the absence of oxygen-containing functional groups in their structures.[23] These could further be explained from the deconvolution analysis of C 1s spectra of untreated and graphene derivative-coated jute fibers.[21] Figure 1g shows a high-resolution C 1s XPS spectrum of untreated jute fibers, which confirms the presence of three main components: C−C bond (~284.5 eV) in cellulosic structure, C−O−C groups (hydroxyl and epoxy, ~286.5 eV), and C═O groups (carbonyl, ~288.3 eV).[39] The C 1s spectrum of GO-coated jute fibers is almost similar to that of untreated jute fibers, shown in Figure 1h. For G 10-coated jute fibers, C 1s is mainly dominated by C−C/C═C (Figure 1i), which is similar to graphene or graphite and in agreement with previous results.[23,40] The G flakes provide less adhesion to cellulosic jute fibers, due to the absence of oxygen-containing functional groups. Fourier transform infrared spectroscopy (FTIR) analysis of untreated and graphene material-treated jute fiber provides further evidence of the removal of hemicellulose after alkali treatment and also the coating with GO and G flakes (Figure S3a,b, Supporting Information).

Interfacial Shear Strength. Interfacial shear strength (IFSS) is one of the key parameters to determine the performance of fiber-reinforced polymer composites. The efficient load transfer from matrix to reinforcement can be achieved by good interfacial bonding at fiber/matrix interface. This can then reduce the stress concentration and improve the overall mechanical properties of composites. There are a number of composite properties that are significantly influenced by IFSS, such as compressive strength and strain to failure, impact properties, damage initiation threshold, fracture toughness, and fatigue life.[41] We use a single-fiber microbond pull-out test to measure IFSS at the fiber/matrix interface. Figure 2a−d shows the optical images of microdroplets used for different treated jute fibers. Figure 2e shows that IFSS values are relatively lower (~4.16 MPa) at the untreated jute fiber/epoxy interface. This may be due to the presence of a waxy cementing layer on the fiber surface, which contains low molecular weight fats, lignin, pectin, and hemicellulose, as discussed earlier. After heat and alkali treatment, the cementing layer is removed, providing a rough fiber surface and better interlocking of the fiber with epoxy resin. Therefore, the IFSS value increases to 7.37 MPa after HA 0.5 treatment, shown in Figure 2e. Previous studies[10,16,42−45] also suggested that the alkali treatment improves the IFSS of jute and other natural fiber composites by 30−140% (Table S4, Supporting Information).

The single-fiber microbond test shows further significant improvement in IFSS after coating of graphene materials onto HA 0.5-treated jute fibers. The coating of GO onto HA 0.5-treated jute fibers enhances IFSS with the increase of GO concentration, shown in Figure 2e. The IFSS of GO 1.0-coated fibers is found to be 14 MPa, which is 245 and 89% more than that of untreated fibers and HA 0.5-treated fibers, respectively, although several previous studies[25,27] reported that the coating with GO improved IFSS of synthetic fiber-reinforced composites by 40−60%. However, this is the first report of such a study on natural fiber composites to the best of our knowledge and the highest reported improvement in IFSS of any fiber-reinforced composites after coating with GO. (Please see the comparison in Table S4, Supporting Information.)

As seen from the XPS analysis (Figure 1h), GO-coated fibers contain a significant amount of oxygen-containing functional groups such as hydroxyl (−OH), epoxide (C−O−C), carbonyl (C═O), and carboxyl (O−C═O). These functional groups interact with the groups of epoxy resin and form a strong mechanical interlocking at the fiber/matrix interface by suitable bonding. Moreover, we use an amine-based hardener to solidify the fiber/epoxy network, which may form C−N bonds through ring opening polymerization.[25,46,47] Furthermore, GO provides strong adhesion and uniform coating on the fiber surface due to the better hydrophilicity of HA 0.5-treated jute fibers. SEM images (Figure 2h−j) of typical

DOI: 10.1021/acsami.8b13018
ACS Appl. Mater. Interfaces 2018, 10, 34502−34512

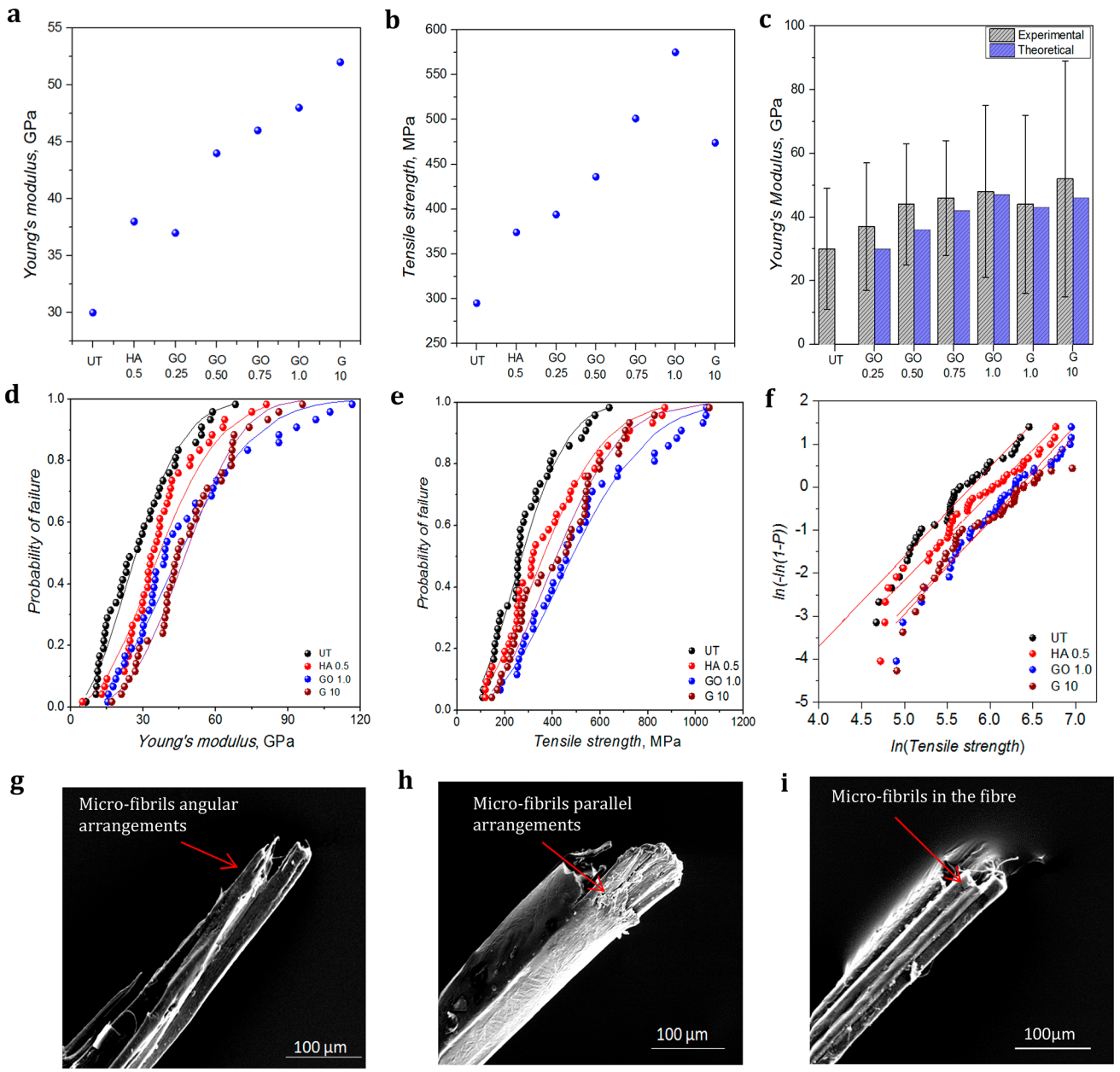

Figure 3. (a) Young's modulus and (b) tensile strength of untreated, GO-treated, and G flake-coated jute fibers; (c) comparative analysis of theoretical and experimental Young's modulus of untreated and graphene-based jute fibers; (d) Young's modulus data fitted to a two-parameter Weibull probability distribution as a function of surface treatment; (e) tensile strength data fitted to a two-parameter Weibull probability distribution as a function surface treatment; (f) ln curves of Weibull parameter plot distribution considering the tensile strength; (g) SEM image of the failure area of untreated jute fiber (X250); (h) SEM image of the failure area of GO-coated jute fiber (X250); and (i) SEM image of the failure area of G flake-coated jute fiber (X250).

microdroplets before and after the microbond test show a strong interface between the jute fiber and the epoxy matrix, as in Figure 2j (circle line). Moreover, the alkali treatment of jute fiber removes the cementing layer to produce a rough surface, which is similar to that observed in the previous study.[16] GO flakes may act as fillers on that rough surface and cluster between the cellulosic chains of fibers, thus forming a strong hydrogen bond and enhancing IFSS at the fiber/matrix interface. In contrast, the coating with 1 wt % G flakes (G 1.0) does not show much improvement in IFSS, may be due to the absence of oxygen-containing functional groups. However, the higher concentration (10 wt %) of G flakes (G 10) improves IFSS of treated jute fibers to 11 ± 5 MPa, which is ~164 and ~65% more than the IFSS of untreated and HA 0.5-treated jute/epoxy composites, respectively. This may be due to the formation of a mechanically interlocked coating of G flakes on the fiber surface, by the diffusion of highly concentrated G flakes into alkali-treated rough and porous jute fiber structure (Figure S1d, Supporting Information).

We use Weibull statistics to analyze the type of failure that happens at the fiber/matrix interface. The cumulative probability of failure is given by the following formula.

$$P = 1 - \exp\left(\left(\frac{\tau_s}{\tau_o}\right)^m\right) \quad (1)$$

DOI: 10.1021/acsami.8b13018
ACS Appl. Mater. Interfaces 2018, 10, 34502−34512

where τ_s is the shear strength, τ_o is the Weibull scale parameter, and m is the Weibull shape parameter. On the basis of the eq 1, a double natural logarithm is taken on both sides, which is shown in eq 2

$$\ln(-\ln(1 - P)) = m \ln(\tau_s - m \ln \tau_o) \quad (2)$$

The Weibull scale parameter and Weibull shape parameter of the untreated and treated fibers to an epoxy resin are calculated by plotting the Weibull probability distribution curves, as shown in Figure 2f,g. The higher number of defects will reduce the Weibull modulus and therefore will result in lower interfacial shear strength of the jute/epoxy composites. We observe that the Weibull modulus of untreated jute fibers is 2.06, which gradually increases to ∼3 with the increase of concentrations after coating of GO onto a jute fiber surface. It indicates that GO flakes are actively working at the interface to reduce any defects present in the fiber. However, this value reduces to 1.87 (Table S5, Supporting Information) for G flakes and shows scattered failure at the interface of jute/epoxy composites.

Tensile Properties. Figure 3a−c shows the effect of graphene material coatings on the tensile properties of single jute fibers (Table S6, Supporting Information). As tensile properties of natural fibers vary largely due to the variations in fiber fineness, we use 50 single fibers for each test. We then plot average results from these 50 samples in Figures 3, S4, and S5, Supporting Information. The values of tensile strength and Young's modulus obtained from mechanical characterization are statistically analyzed using a two-parameter Weibull distribution (eqs S1−S4, Supporting Information). The tensile modulus and strength of untreated fibers are found to be ∼30 GPa and ∼295 MPa, respectively, which are similar to those reported in previous studies.[5,48]

After HA 0.5 treatment, the tensile modulus and strength is increased by 26 and 26.5%, respectively, as in Figure 3a,b. However, the breaking force and extension at break is reduced by 23.5 and 11%, respectively (Table S6, Supporting Information). This could possibly be because of voids that are created due to the irregular removal of impurities from the fiber surface by heat and alkali treatment (Figure S1b, Supporting Information). Several previous studies reported the effect of alkali treatment on jute fibers[9,11,15] and indicate that the tensile properties of jute fiber depend on its diameter and cellulose content. NaOH (alkali) solution has a strong bleaching effect; thus, it removes impurities from the fiber surface. The alkali treatment also degrades hemicellulose from the interfibrillar region and removes lignin from the intercellular region of jute fibers, causing separation of fibers from the cell and reduction in fiber diameter.[11] They reported that the removal of a significant amount of lignin could be responsible for the reduction in breaking force and breaking extension of the jute fiber. Moreover, when the tensile force is applied, the intercell of the jute fiber can shear easily at lower force and extend due to the removal of lignin. Figure 3g shows the broken surface of an untreated single jute fiber and demonstrates an irregular pattern of breakage due to the angular arrangement of microfibrills. Baley and his co-workers[49] observed a similar series of events in flax fibers where they explained that the slipping of these microfibrils happens during axial loading due to the local shear stress that is developed between them.

Further treatment with graphene materials significantly improves Young's modulus and the tensile strength of jute fibers. After coating GO (1 wt %) onto jute fibers, Young's modulus increases from 30 to 48 GPa and the tensile strength from 295 to 575 MPa, which are 60 and 94%, respectively, more than those with the untreated jute fiber. The enhanced mechanical properties of GO-coated jute fiber could again be due to the strong adhesion between functional groups of GO and those of HA 0.5-treated jute fibers via suitable bonding. Also, GO flakes possess an extremely high modulus that could possibly stiffen the jute fiber and remove stress concentrations on the fiber surface during tensile loading, thus enhancing the tensile properties of jute fiber. Moreover, the SEM image of a GO-coated jute fiber shows that pores of cellulose microfibrils are filled with GO flakes (Figure S1c, Supporting Information), which increases fiber packing (Figure 3h) and provides better tensile properties. We also observe that the tensile properties of jute fibers improve with the increase in GO concentrations, as in Figure 3a,b.

Similarly, the coating with higher concentration of G flakes (G 10) on HA 0.5-treated jute fibers increases Young's modulus and tensile strength by ∼73% (to 52 GPa) and ∼60% (to 474 MPa), respectively, more than that of untreated jute fibers. The improvement in tensile strength from G flakes is lower than that of GO-coated fibers. However, Young's modulus of G flake (G 10)-coated jute fibers is higher than that of any other coated fiber, probably due to the uniform deposition of a large amount of flakes on the fiber surface, as evident from SEM image, in Figures 1c and S1d, Supporting Information. We also compare diameter versus tensile properties of untreated and treated jute fibers (Figure S4, Supporting Information). It shows that the increase of diameter has an effect on both Young's modulus and tensile strength of jute fiber.

We use a well-established Halpin−Tsi model[50,51] to theoretically predict the reinforcing mechanism of coated jute fibers with graphene materials. The modulus of the graphene-based jute fibers can be calculated from the following equations.

$$E_C = \frac{3}{8}\frac{(1 + \xi\eta_L V_G)}{(1 - \eta_L{}^* V_G)} \times E_M + = \frac{5}{8}\frac{(1 + \varepsilon\eta_W V_G)}{(1 - \eta_W V_G)} \times E_M \quad (3)$$

$$\eta_L = \frac{(E_G/E_M - 1)}{(E_G/E_M + \xi)} \quad (4)$$

$$\eta_W = \frac{(E_G/E_M - 1)}{(E_G/E_M + 2)} \quad (5)$$

$$\xi = 2\frac{(w + l)/2}{t} \quad (6)$$

$$V_G = \frac{W_G}{W_G + (\rho_G/\rho_M)(1 - W_G)} \quad (7)$$

where E_C is the tensile modulus of graphene-based jute fibers, V_G is the effective volume fraction of graphene-based jute fibers, E_G and E_M are the effective modulus of graphene and fiber, respectively. The parameter ξ depends on the size and shape of the graphene used in this study and is determined by eq 6. L, W, and t represent the average graphene length, width, and thickness. W_G is the weight fraction of graphene and ρ_G and ρ_M are the density of graphene and jute fiber, respectively.

DOI: 10.1021/acsami.8b13018
ACS Appl. Mater. Interfaces 2018, 10, 34502−34512

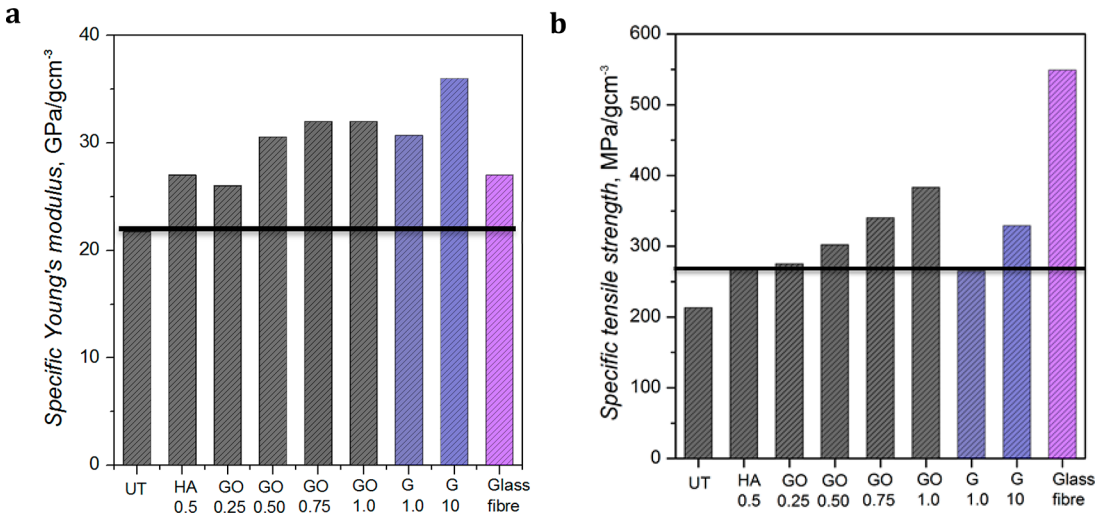

Figure 4. Comparison of specific tensile properties: (a) specific Young's modulus and (b) specific tensile strength of untreated and graphene material-treated jute fibers with glass fiber (glass fiber value taken from the literature[62]).

Table 1. Tensile Properties of Natural Fiber before and after Modification Reported in the Literature[a]

		Young's modulus, GPa			Tensile strength, MPa			
fibers	treatment	before treatment	after treatment	change %	before treatment	after treatment	change %	reference
jute	NaOH 0.32%	17	14	−17.64	475	400	−15.78	15
jute	NaOH 1%	—	—	—	250	360	+44	8
jute	NaOH 5% + silane 5%	—	—	—	550	540	−1.82	52
jute	nano-SiO_2—	21.5	23.1	+7.44	471.8	501.2	+6.23	53
flax	NaOH—	—	—	—	934	423	−54.7	54
flax (y)	nano TiO_2—	—	—	—	5545	6344	+14.4	55
flax	nano TiO_2 (∼4%)	30.6	31.9	+4.24	464.0	480.6	+3.57	31
flax	CNT (∼2%)	32	30	−6.25	400	300	−25	56
sisal	SNC—	—	—	—	512	451	−11.91	57
sisal	NaOH 2% + silane 2%	12.2	7.5	−38.52	345	138	−60	58
kenaf	NaOH 6%	40.32	37.82	−6.2	501.56	483.16	−3.66	59
jute	GO 1%	30	48	+60	295	578	+95.93	this study
	G 10%	30	52	+73.33	295	474	+60.67	

[a]SNC, starch nanocrystals; CNT, carbon nanotube'; — information not given; Y, yarn.

The parameters used for graphene (such as length, width, thickness, modulus, and density) in this study are tabulated in Table S7, Supporting Information. We use eqs 3−7 to predict the theoretical values of Young's modulus and then compare with the experimental results, in Figure 3c. As seen from the results, Young's modulus increases with the increase of GO concentrations both in experimental and theoretical results. Moreover, the predicted tensile modulus of graphene-coated fibers (HA−GO and HA−G) is slightly (∼6%) less than the experimental results, which is acceptable, as explained by Tian et al.[50] They mention that the tensile modulus of graphene-based fibers is lower due to the wrinkled structure of graphene; whereas we consider a rectangular shape for graphene flakes in our theoretical calculation. On the basis of the results obtained, we could say that the Halpin−Tsi model is an effective way to predict the tensile modulus of graphene-based fibers.

Like IFSS, we carry out statistical analysis for jute fiber's tensile properties as well, as they exhibit scattered results for tensile strength and Young's modulus. We again use two-parameter (scale parameter, α and shape parameter, β) Weibull distribution for this analysis (Table S6, Supporting Information), where α predicts experimental results and β indicates the modulus of Weibull distribution known as Weibull modulus. Figure 3d,e shows the Weibull probability distribution plots for treated and untreated jute fibers considering the Young's modulus and strength, respectively. Both distributions are shifted significantly from the left to right side after fibers are treated with graphene materials (GO and G). We obtain the Weibull modulus from ln curves of both Young's modulus and tensile strength, Figures 3f and S5b, Supporting Information. The untreated jute fibers provide a lower value of Weibull modulus (∼1.86), which indicates a high scattering in the tensile properties of untreated jute fiber due to the non-homogenous nature of the fiber. However, the Weibull modulus increases up to ∼2.95 after GO grafting, which may be due to the better bonding between fibers and GO, as explained earlier. However, the Weibull modulus is reduced (∼1.67) for jute fibers treated with G flakes.

We compare the specific properties (the ratio of the experimental value and density) of jute fiber with glass fibers. Figure 4a,b shows the comparison of the specific Young's modulus and the specific tensile strength of jute and glass fibers, respectively (Table S8, Supporting Information). Specific properties of alkali-treated fiber are almost equal to those of glass fiber. After graphene-based treatments, we achieve 15.6 and 18.5% higher specific modulus for GO-coated

DOI: 10.1021/acsami.8b13018
ACS Appl. Mater. Interfaces 2018, 10, 34502−34512

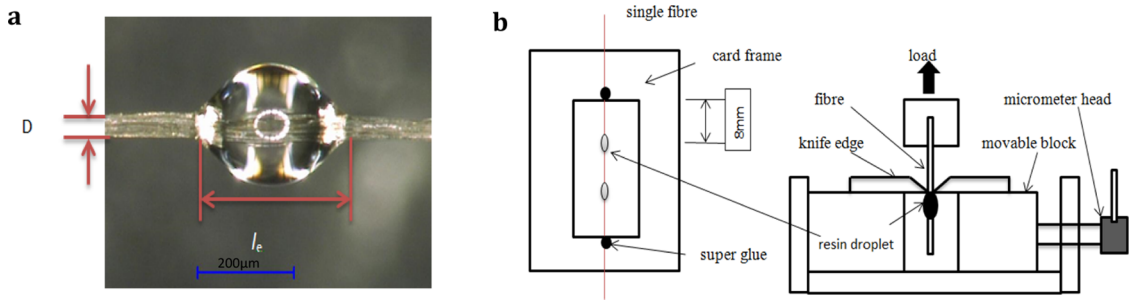

Figure 5. Microdroplet preparation: (a) microdroplet of jute/epoxy specimen and (b) schematic diagram of a microbond testing device using a microvise.

(32 GPa/g/cm^3) and G 10 (36 GPa/g/cm^3)-coated fibers, respectively, than that of glass fiber (27 GPa/g/cm^3). Although the specific tensile strength of glass fiber is still higher than that of GO- and G-treated fibers, graphene material treatment on jute fibers shows a significant improvement in specific strength after grafting with GO and G flakes. We finally compare obtained results (the tensile properties) in this study with the recently published works, in Table 1. Although direct comparison may be difficult as all results collected from the literature were obtained under different experimental conditions. Table 1 shows a brief comparison between the results obtained with various surface treatments on jute and other natural fibers. The traditional alkali treatment followed by nanomodification of jute fiber in the literature does not show a significant improvement in the tensile properties. However, jute fiber treated by GO and graphene flakes in our study shows a fairly large increment in the both Young's modulus (~73.33% for G flakes) and tensile strength (~95.9% for the GO-treated jute fibers) than the untreated fiber.

CONCLUSIONS

We report grafting of graphene oxides and graphene flakes onto jute fibers to produce high-performance graphene-based natural fiber composites. The graphene material-coated jute fibers thus produced exhibit significant increase in the tensile and interfacial properties and comparable specific properties to those of glass fibers. We believe that our graphene-based high-performance natural fiber composite is an important step toward replacing synthetic composites for some real world applications.

EXPERIMENTAL METHODS

Materials. The plant material (*Corchorus Olitorious*) known as "Tossa white jute" was obtained from Bangladesh, cultivated on the sandy loam plateau in the Northeast of Dhaka. The sample was cultivated from February to May in 2015. The annual rainfall of this area is 500−1500 mm and the temperature ranges from 20 to 33 °C. The content of long fibers in the bundles is 98−99 wt %, whereas the remaining 1−2 wt % is shives (cortical tissues and dust). The untreated long jute fiber has a golden color with an average length and diameter of 2.9 m and 0.059 mm, respectively. Analytical grade sodium hydroxide (NaOH) pellets (product no: 10502731) were purchased from Fisher Scientific, U.K. EL2 Epoxy Laminating Resin and AT30 Epoxy Hardener were purchased from Easy Composites, U.K. The natural flake graphite (average lateral size 50 mm) was kindly supplied by Graphexel Limited, U.K. Sodium deoxycholate (SDC) powder, potassium permanganate ($KMnO_4$), sulfuric acid (H_2SO_4, ~99%), and hydrogen peroxide (H_2O_2, ~30%) were purchased from Sigma-Aldrich, U.K.

Graphene Material Synthesis. Our previously reported method was followed to prepare microfluidized graphene flakes (G).[23] Briefly, 10 g of SDC and 50 g of flake graphite are added into a glass bottle and mixed with 500 mL of deionized (DI) water and sonicated for 30 min. This mixture is then passed through "Z-type" microfluidic channels of 200 and 87 mm diameter with diamond construction of a Microfluidizer (M-110P Microfluidizer, Microfluidics Corp) at high pressure, which allows the exfoliation of graphite to few-layer graphene (G Flakes) under a high shear rate (108 s^{-1}). A modified Hummer's method that was described elsewhere was used to prepare graphene oxide (GO) in water.[60]

Alkali Treatment and Graphene Material Coating. Untreated jute fibers were washed with deionized (DI) water after cutting into 30 cm long pieces, and they were then dried at 80 °C until a constant weight was achieved. These fibers were treated in warm water at 60 °C for 60 min and then boiled at 100 °C for 30 min. The weight of fibers was reduced by 6 wt %, labeled as heat treated (HT) fibers. After these cleaning procedures, HT jute fibers were dipped in 0.5 wt % NaOH solutions with a 1:50 material-to-liquor ratio (M/L) to remove hemicelluloses. The fibers obtained after two cycles of alkali treatment are termed as HA 0.5 and undergo losses of almost similar weight ~6 wt %, as reported in previous work.[8]

HA 0.5 jute fibers were then coated with GO and G flakes using a simple dip coating for 30 min and subsequently dried at 80 °C for 30 min. The various concentrations of GO such as 0.25, 0.5, 0.75, and 1 wt % were used to prepare GO-coated samples: GO 0.25, GO 0.5, GO 0.75, and GO 1.0, respectively. Graphene flakes (1 and 10 wt %, G 1 and G 10) were used to compare the performance with GO-coated fibers. The concentrations of GO on the weight of jute fibers (owf %) were calculated as 0.34, 0.71, 0.97, and 1.54 wt % for GO 0.25, GO 0.50, GO 0.75, and GO 1, respectively. Also, the concentrations of graphene flakes (G 1 and G 10) were obtained as 1.53 and 2.41 wt %, respectively, on the weight of jute fibers (owf %).

Characterization. A Philip XL-30 field emission gun scanning electron microscope (SEM) was used to analyze the surface topography of the treated and untreated jute fibers. The surface characteristics of untreated and graphene material-coated jute fibers was analyzed using a Kratos axis X-ray photoelectron spectroscopy (XPS) system and Fourier transform infrared spectroscopy (FTIR). The thermal decomposition of untreated and coated jute fibers from room temp to 1000 °C in a nitrogen atmosphere at 10 °C/min heating rate was analyzed using a TA instrument (TGA Q5000, U.K.).

Tensile Testing of Elementary Fibers. The graphene material-coated jute fibers were fibrillated using an inhouse handmade comb (Figure S6a, Supporting Information) and mixed together. The elementary fibers are separated from the fibrillated fiber bundle (technical fiber) (Figure S7, Supporting Information). These were then mounted on a paper frame using superglue and left overnight to be cured properly. The average fiber diameter was measured from five measurements for every fiber using a digital microscope (Keyence digital microscope VHX-500F, U.K.). These fiber samples were then kept in a standard laboratory atmosphere (55% relative humidity and 20 ± 2 °C) for 24 h before further testing. A Zwick tensile testing machine (Zwick/Roell, U.K.) with a load cell of 20 N was used to measure the uniaxial tensile strength and elongation at break of jute fibers. A gauge length of 20 mm was used with a crosshead speed of 2

DOI: 10.1021/acsami.8b13018
ACS Appl. Mater. Interfaces 2018, 10, 34502−34512

mm/min according to ASTM standard D3822-01.[8] The moduli of the fibers were calculated from the slope at 0.1−0.3% strain of the fiber.

Single-Fiber Microbond Test. As previously reported,[61] all elementary fibers with a length between 30 and 50 mm were separated manually for single-fiber microbond test. Elementary fibers were then attached to a window of the paper card frame (25 × 10 mm) using superglue with a very negligible amount of tension (Figure S6b, Supporting Information). Microdroplets of epoxy resin were created using a glass fiber, as in Figure 5a, and then applied to test specimens and cured at room temperature. A Keyence digital microscope (VHX-500F, U.K.) with 200× magnification was used to measure the diameter of the fiber and the embedded length of the resin droplets. A one-side rotating microvise with two sharp blade edges was used to perform the test, shown in Figure 5b. The embedded length by resin droplet was kept between 200 and 300 μm to avoid fiber breakage during the test. The test was performed on a Zwick tensile testing machine (Zweich/Roell, U.K.) equipped with a load cell of the 20 N at a loading rate of 0.25 mm/min, and the force−displacement curve was recorded. The average IFSS was calculated from the data recorded from 30 samples.

The IFSS is calculated from the maximum pull-out force (F), the microdroplet length (l_e), and the fiber diameter (D) using the following eq 8.

$$\tau_{\mathrm{IFFS}} = \frac{F}{\pi D l_e} \tag{8}$$

■ ASSOCIATED CONTENT

Supporting Information

The Supporting Information is available free of charge on the ACS Publications website at DOI: 10.1021/acsami.8b13018.

Comparative advantages of natural fibers over synthetic fibers and comparison of their physical and mechanical properties; microscopic (SEM and optical) images of untreated, alkali-treated, and graphene material-coated jute fibers; thermal and chemical (FTIR) analysis of untreated and treated jute fibers; comparative IFSS results obtained in the literature and our study; mechanical properties of untreated and treated jute fibers with their statistical values; typical stress−strain curves and Weibull distribution plots; size and thickness distribution of graphene materials used in this study; specific properties of untreated and treated jute fibers; and fiber preparation, treatments, and testings with images of the experimental setup (PDF)

■ AUTHOR INFORMATION

Corresponding Authors

*E-mail: mdnazmul.karim@manchester.ac.uk (N.K.).
*E-mail: prasad.potluri@manchester.ac.uk (P.P.).

ORCID

Nazmul Karim: 0000-0002-4426-8995

Author Contributions

⊥F.S. and N.K. contributed equally to this work.

Author Contributions

The manuscript was written through contributions of all authors. All authors have given approval to the final version of the manuscript.

Notes

The authors declare no competing financial interest.

■ ACKNOWLEDGMENTS

Authors kindly acknowledge Commonwealth Scholarship Council, U.K. and the Government of Bangladesh for the PhD funding of Forkan Sarker and Shaila Afroj, respectively. This work was supported by EU Graphene Flagship Program, European Research Council Synergy Grant Hetero2D, the Royal Society, and Engineering and Physical Sciences Research Council, U.K. (Grant Number: EP/N010345/1, 2015).

■ REFERENCES

(1) Alkbir, M.; Sapuan, S.; Nuraini, A.; Ishak, M. R. Fiber Properties and Crashworthiness Parameters of Natural Fiber-Reinforced Composite Structure: A Literature Review. *Compos. Struct.* **2016**, *148*, 59−73.

(2) Lau, K.-t.; Hung, P.-y.; Zhu, M. H.; Hui, D. Properties of Natural Fibre Composites for Structural Engineering Applications. *Composites, Part B* **2018**, *136*, 222−233.

(3) Roe, P. J.; Ansell, M. P. Jute-Reinforced Polyester Composites. *J. Mater. Sci.* **1985**, *20*, 4015−4020.

(4) Koronis, G.; Silva, A.; Fontul, M. Green Composites: A Review of Adequate Materials for Automotive Applications. *Composites, Part B* **2013**, *44*, 120−127.

(5) Gassan, J.; Bledzki, A. K. Possibilities for Improving the Mechanical Properties of Jute/epoxy Composites by Alkali Treatment of Fibres. *Compos. Sci. Technol.* **1999**, *59*, 1303−1309.

(6) Sen, M.; Mukherjee, R. The Structure of Jute, Part1,-The X-Ray Diffraction Pattern. *J. Text. Inst., Proc.* **1952**, *43*, 114−121.

(7) Gassan, J.; Bledzki, A. K. Alkali Treatment of Jute Fibers: Relationship between Structure and Mechanical Properties. *J. Appl. Polym. Sci.* **1999**, *7*, 623−629.

(8) Roy, A.; Chakraborty, S.; Kundu, S. P.; Basak, R. K.; Majumder, S. B.; Adhikari, B. Improvement in Mechanical Properties of Jute Fibres through Mild Alkali Treatment as Demonstrated by Utilisation of the Weibull Distribution Model. *Bioresour. Technol.* **2012**, *107*, 222−228.

(9) Saha, P.; Manna, S.; Chowdhury, S. R.; Sen, R.; Roy, D.; Adhikari, B. Enhancement of Tensile Strength of Lignocellulosic Jute Fibers by Alkali-Steam Treatment. *Bioresour. Technol.* **2010**, *101*, 3182−3187.

(10) Cai, M.; Takagi, H.; Nakagaito, A. N.; Li, Y.; Waterhouse, G. I. N. Effect of Alkali Treatment on Interfacial Bonding in Abaca Fiber-Reinforced Composites. *Composites, Part A* **2016**, *90*, 589−597.

(11) Mukherjee, A.; Ganguly, P. K.; Sur, D. Structural Mechanics of Jute: The Effects of Hemicellulose or Lignin Removal. *J. Text. Inst.* **1993**, *84*, 348−353.

(12) Bledzki, A.; Gassan, J. Composites Reinforced with Cellulose Based FIbre. *Prog. Polym. Sci.* **1999**, *24*, 221−274.

(13) De Albuquerque, A. C.; Joseph, K.; Hecker De Carvalho, L.; D'Almeida, J. R. M. Effect of Wettability and Ageing Conditions on the Physical and Mechanical Properties of Uniaxially Oriented Jute-Roving-Reinforced Polyester Composites. *Compos. Sci. Technol.* **2000**, *60*, 833−844.

(14) Roy, M. Mechanical Prooperties of Jute II: The Study of Chemically Treated Fibres. *J. Text. Inst., Trans.* **1953**, *44*, T44−T52.

(15) Mwaikambo, L. Y. Tensile Properties of Alkalised Jute Fibres. *BioResources* **2009**, *4*, 566−588.

(16) Doan, T.-T.-L.; Brodowsky, H.; Mäder, E. Jute Fibre/epoxy Composites: Surface Properties and Interfacial Adhesion. *Compos. Sci. Technol.* **2012**, *72*, 1160−1166.

(17) Demir, A.; Seki, Y.; Bozaci, E.; Sarikanat, M.; Erden, S.; Sever, K.; Ozdogan, E. Effect of the Atmospheric Plasma Treatment Parameters on Jute Fabric: The Effect on Mechanical Properties of Jute Fabric/Polyester Composites. *J. Appl. Polym. Sci.* **2011**, *121*, 634−638.

(18) Sever, K.; Erden, S.; Gülec, H. A.; Seki, Y.; Sarikanat, M. Oxygen Plasma Treatments of Jute Fibers in Improving the Mechanical Properties of jute/HDPE Composites. *Mater. Chem. Phys.* **2011**, *129*, 275−280.

DOI: 10.1021/acsami.8b13018
ACS Appl. Mater. Interfaces 2018, 10, 34502−34512

(19) Chen, H.; Müller, M. B.; Gilmore, K. J.; Wallace, G. G.; Li, D. Mechanically Strong, Electrically Conductive, and Biocompatible Graphene Paper. *Adv. Mater.* **2008**, *20*, 3557−3561.
(20) Karim, N.; Afroj, S.; Malandraki, A.; Butterworth, S.; Beach, C.; Rigout, M.; Novoselov, K. S.; Casson, A. J.; Yeates, S. G. All Inkjet-Printed Graphene-Based Conductive Patterns for Wearable E-Textile Applications. *J. Mater. Chem. C* **2017**, *5*, 11640−11648.
(21) Karim, N.; Afroj, S.; Tan, S.; He, P.; Fernando, A.; Carr, C.; Novoselov, K. S. Scalable Production of Graphene-Based Wearable E-Textiles. *ACS Nano* **2017**, *11*, 12266−12275.
(22) Abdelkader, A. M.; Karim, N.; Vallés, C.; Afroj, S.; Novoselov, K. S.; Yeates, S. G. Ultraflexible and Robust Graphene Supercapacitors Printed on Textiles for Wearable Electronics Applications. *2D Mater.* **2017**, *4*, No. 035016.
(23) Karim, N.; Zhang, M.; Afroj, S.; Koncherry, V.; Potluri, P.; Novoselov, K. S. Graphene-Based Surface Heater for de-Icing Applications. *RSC Adv.* **2018**, *8*, 16815−16823.
(24) Chen, J.; Zhao, D.; Jin, X.; Wang, C.; Wang, D.; Ge, H. Modifying Glass Fibers with Graphene Oxide: Towards High-Performance Polymer Composites. *Compos. Sci. Technol.* **2014**, *97*, 41−45.
(25) Zhang, X.; Fan, X.; Yan, C.; Li, H.; Zhu, Y.; Li, X.; Yu, L. Interfacial Microstructure and Properties of Carbon Fiber Composites Modified with Graphene Oxide. *ACS Appl. Mater. Interfaces* **2012**, *4*, 1543−1552.
(26) Arfaoui, M. A.; Dolez, P. I.; Dubé, M.; David, É. David. Development and Characterization of a Hydrophobic Treatment for Jute Fibres Based on Zinc Oxide Nanoparticles and a Fatty Acid. *Appl. Surf. Sci.* **2017**, *397*, 19−29.
(27) Chen, L.; Wei, F.; Liu, L.; Cheng, W.; Hu, Z.; Wu, G.; Du, Y.; Zhang, C.; Huang, Y. Grafting of Silane and Graphene Oxide onto PBO Fibers: Multifunctional Interphase for Fiber/polymer Matrix Composites with Simultaneously Improved Interfacial and Atomic Oxygen Resistant Properties. *Compos. Sci. Technol.* **2015**, *106*, 32−38.
(28) Xiong, R.; Grant, A. M.; Ma, R.; Zhang, S.; Tsukruk, V. V. *Naturally-Derived Biopolymer Nanocomposites: Interfacial Design, Properties and Emerging Applications*; Materials Science and Engineering R: Reports; Elsevier, 2018; pp 1−41.
(29) Xiong, R.; Kim, H. S.; Zhang, L.; Korolovych, V. F.; Zhang, S.; Yingling, Y. G.; Tsukruk, V. V. Wrapping Nanocellulose Nets around Graphene Oxide Sheets. *Angew. Chem.* **2018**, *130*, 8644−8649.
(30) Xiong, R.; Hu, K.; Grant, A. M.; Ma, R.; Xu, W.; Lu, C.; Zhang, X.; Tsukruk, V. V. Ultrarobust Transparent Cellulose Nanocrystal-Graphene Membranes with High Electrical Conductivity. *Adv. Mater.* **2016**, *28*, 1501−1509.
(31) Wang, H.; Xian, G.; Li, H. Grafting of Nano-TiO_2 onto Flax Fibers and the Enhancement of the Mechanical Properties of the Flax Fiber and Flax Fiber/epoxy Composite. *Composites, Part A* **2015**, *76*, 172−180.
(32) Mwaikambo, L. Y.; Ansell, M. P. Chemical Modification of Hemp, Sisal, Jute, and Kapok Fibers by Alkalization. *J. Appl. Polym. Sci.* **2002**, *84*, 2222−2234.
(33) Byeon, J. M.; Nam, G. B.; Kim, J. W.; Kim, B. S.; Song, J. I. Surface Treatment Influence on the Mechanical Behavior of Jute Fiber Reinforced Composites. *Adv. Mater. Res.* **2011**, *410*, 122−125.
(34) Kumar J, P.; Sugunakar, A.; Nagaraj, C. Effect of Alkali Treatment on Mechanical Properties of Agave Fibre Reinforced Polymer Composites. *IOSR J. Mech. Civ. Eng.* **2016**, *16*, 37−43.
(35) Liu, M.; Meyer, A. S.; Fernando, D.; Silva, D. A. S.; Daniel, G.; Thygesen, A. Effect of Pectin and Hemicellulose Removal from Hemp Fibres on the Mechanical Properties of Unidirectional Hemp/epoxy Composites. *Composites, Part A* **2016**, *90*, 724−735.
(36) Papageorgiou, D. G.; Terzopoulou, Z.; Fina, A.; Cuttica, F.; Papageorgiou, G. Z.; Bikiaris, D. N.; Chrissafis, K.; Young, R. J.; Kinloch, I. A. Enhanced Thermal and Fire Retardancy Properties of Polypropylene Reinforced with a Hybrid Graphene/glass-Fibre Filler. *Compos. Sci. Technol.* **2018**, *156*, 95−102.
(37) Alongi, J.; Malucelli, G. Thermal Stability, Flame Retardancy and Abrasion Resistance of Cotton and Cotton-Linen Blends Treated by Sol-Gel Silica Coatings Containing Alumina micro or Nano-Particles. *Polym. Degrad. Stab.* **2013**, *98*, 1428−1438.
(38) Kandola, B.; Sarker, F.; Luangtriratana, P.; Myler, P. Thermal Protection of Carbon Fiber-Reinforced Composites by Ceramic Particles. *Coatings* **2016**, *6*, 22.
(39) Erdoğan, U. H.; Seki, Y.; Aydoğdu, G.; Kutlu, B.; Akşit, A. Effect of Different Surface Treatments on the Properties of Jute. *J. Nat. Fibers* **2016**, *13*, 158−171.
(40) Abdelkader, A. M.; Kinloch, I. A. Mechanochemical Exfoliation of 2D Crystals in Deep Eutectic Solvents. *ACS Sustainable Chem. Eng.* **2016**, *4*, 4465−4472.
(41) Godara, A.; Gorbatikh, L.; Kalinka, G.; Warrier, A.; Rochez, O.; Mezzo, L.; Luizi, F.; van Vuure, A. W.; Lomov, S. V.; Verpoest, I. Interfacial Shear Strength of a Glass Fiber/epoxy Bonding in Composites Modified with Carbon Nanotubes. *Compos. Sci. Technol.* **2010**, *70*, 1346−1352.
(42) Pisanova, E.; Mäder, E. Acid−base Interactions and Covalent Bonding at a Fiber−matrix Interface: Contribution to the Work of Adhesion and Measured Adhesion Strength. *J. Adhes. Sci. Technol.* **2000**, *14*, 415−436.
(43) Nam, T. H.; Ogihara, S.; Tung, N. H.; Kobayashi, S. Effect of Alkali Treatment on Interfacial and Mechanical Properties of Coir Fiber Reinforced Poly(butylene Succinate) Biodegradable Composites. *Composites, Part B* **2011**, *42*, 1648−1656.
(44) Orue, A.; Jauregi, A.; Peña-Rodriguez, C.; Labidi, J.; Eceiza, A.; Arbelaiz, A. The Effect of Surface Modifications on Sisal Fiber Properties and Sisal/poly (lactic Acid) Interface Adhesion. *Composites, Part B* **2015**, *73*, 132−138.
(45) Van de Weyenberg, I.; Chi Truong, T.; Vangrimde, B.; Verpoest, I. Improving the Properties of UD Flax Fibre Reinforced Composites by Applying an Alkaline Fibre Treatment. *Composites, Part A* **2006**, *37*, 1368−1376.
(46) Wang, S.; Chia, P. J.; Chua, L. L.; Zhao, L. H.; Png, R. Q.; Sivaramakrishnan, S.; Zhou, M.; Goh, R. G.-S.; Friend, R. H.; Wee, A. T.-S.; Ho, P. K.-H. Band-like Transport in Surface-Functionalized Highly Solution-Processable Graphene Nanosheets. *Adv. Mater.* **2008**, *20*, 3440−3446.
(47) Yang, H.; Shan, C.; Li, F.; Zhang, Q.; Han, D.; Niu, L. Convenient Preparation of Tunably Loaded Chemically Converted Graphene Oxide/epoxy Resin Nanocomposites from Graphene Oxide Sheets through Two-Phase Extraction. *J. Mater. Chem.* **2009**, *19*, 8856.
(48) Virk, A. S.; Hall, W.; Summerscales, J. Tensile Properties of Jute Fibres. *Mater. Sci. Technol.* **2009**, *25*, 1289−1295.
(49) Baley, C.; Le Duigou, a; Bourmaud, a; Davies, P. Influence of Drying on the Mechanical Behaviour of Flax Fibres and Their Unidirectional Composites. *Composites, Part A* **2012**, *43*, 1226−1233.
(50) Tian, M.; Qu, L.; Zhang, X.; Zhang, K.; Zhu, S.; Guo, X.; Han, G.; Tang, X.; Sun, Y. Enhanced Mechanical and Thermal Properties of Regenerated Cellulose/graphene Composite Fibers. *Carbohydr. Polym.* **2014**, *111*, 456−462.
(51) Rafiee, M. A.; Rafiee, J.; Wang, Z.; Song, H.; Yu, Z. Z.; Koratkar, N. Enhanced Mechanical Properties of Nanocomposites at Low Graphene Content. *ACS Nano* **2009**, *3*, 3884−3890.
(52) Zafar, M. T.; Maiti, S. N.; Ghosh, A. K. Effect of Surface Treatments of Jute Fibers on the Microstructural and Mechanical Responses of Poly(lactic Acid)/jute Fiber Biocomposites. *RSC Adv.* **2016**, *6*, 73373−73382.
(53) Liu, X.; Cui, Y.; Hao, S.; Chen, H. Influence of Depositing Nano-SiO2particles on the Surface Microstructure and Properties of Jute Fibers via in Situ Synthesis. *Composites, Part A* **2018**, *109*, 368−375.
(54) Lefeuvre, A.; Duigou, A. L.; Bourmaud, A.; Kervoelen, A.; Morvan, C.; Baley, C. Analysis of the Role of the Main Constitutive Polysaccharides in the Flax Fibre Mechanical Behaviour. *Ind. Crops Prod.* **2015**, *76*, 1039−1048.
(55) Foruzanmehr, M.; Vuillaume, P. Y.; Robert, M.; Elkoun, S. The Effect of Grafting a Nano-TiO_2 Thin Film on Physical and Mechanical Properties of Cellulosic Natural Fibers. *Mater. Des.* **2015**, *85*, 671−678.

DOI: 10.1021/acsami.8b13018
ACS Appl. Mater. Interfaces 2018, 10, 34502−34512

(56) Li, Y.; Chen, C.; Xu, J.; Zhang, Z.; Yuan, B.; Huang, X. Improved Mechanical Properties of Carbon Nanotubes-Coated Flax Fiber Reinforced Composites. *J. Mater. Sci.* **2015**, *50*, 1117−1128.
(57) Chang, Y.; Sun, T.; Fan, C.; Zhou, X. The Effect of Surface Modification on the Properties of Sisal Fiber and Improvement of Interfacial Adhesion in Sisal / Starch Composites Induced by Starch Nanocrystals. *Compos. Interfaces* **2018**, *25*, 981−994.
(58) Orue, A.; Jauregi, A.; Unsuain, U.; Labidi, J.; Eceiza, A.; Arbelaiz, A. The Effect of Alkaline and Silane Treatments on Mechanical Properties and Breakage of Sisal Fibers and Poly(lactic Acid)/sisal Fiber Composites. *Composites, Part A* **2016**, *84*, 186−195.
(59) Fiore, V.; Di Bella, G.; Valenza, A. The Effect of Alkaline Treatment on Mechanical Properties of Kenaf Fibers and Their Epoxy Composites. *Composites, Part B* **2015**, *68*, 14−21.
(60) Hummers, W. S.; Offeman, R. E. Preparation of Graphitic Oxide. *J. Am. Chem. Soc.* **1958**, *80*, 1339.
(61) Yang, L.; Thomason, J. L. Interface Strength in Glass Fibre−polypropylene Measured Using the Fibre Pull-out and Microbond Methods. *Composites, Part A* **2010**, *4*, 1077−1083.
(62) Hull, D.; Clyne, T. *An Introduction to Composite Materials*; Cambridge university press, 1996.

DOI: 10.1021/acsami.8b13018
ACS Appl. Mater. Interfaces 2018, 10, 34502−34512